Eksergi
Chemical Engineering Journal
Vol 23, No. 2. 2026

ISSN: 1410-394X
e-ISSN: 2460-8203

Characterization of Polylactic Acid/Chitosan/Cellulose Nanofibers for Wound Dressing Applications

Belinda Laulista[1*], Desy Miftachul[1], Lilik Suprianti[1*], Tri Widjaja[2], Aisyah Alifatul Zahidah Rohmah[1], Citra Yulia Sari[2]

[1]*Chemical Engineering Department, Universitas Pembangunan Nasional "Veteran" Jawa Timur, Surabaya, 60294, Indonesia*

[2]*Chemical Engineering Department, Sepuluh Nopember Institute of Technology, 60111, Indonesia*

Article history:

Submitted 13 February 2026
Revision 4 April 2026
Accepted 8 April 2026
Online 27 April 2026

ABSTRACT: Effective wound care requires dressing materials that provide physical protection while actively encouraging tissue regeneration. This research investigates the development and characterization of biocomposite nanofiber membranes composed of polylactic acid (PLA), chitosan, and cellulose, synthesized via the electrospinning method at an optimized operating voltage of 20 kV. The study aimed to identify the optimal material ratio that balances mechanical durability with surface wettability. Comprehensive evaluations included Scanning Electron Microscopy (SEM), Fourier Transform Infrared (FTIR), water contact angle (WCA) measurements, and mechanical testing. The results demonstrate that the integration of chitosan and cellulose significantly refined fiber morphology and wettability. The optimal variant with a composition of 90:5:5 wt.% (PLA:chitosan:cellulose) achieved a WCA of 98.64°, indicating that the hydrophobicity was maintained relative to pure PLA. M orphologically, the composite fibers were uniform and bead-less, with a mean diameter reduction of 36.2% (from 517.12 nm in pure PLA to 329.68 nm). FTIR spectra confirmed successful component incorporation through characteristic amide and hydroxyl bands. Mechanically, the composite membrane exhibited a superior synergy between strength and flexibility, achieving a yield strength of 0.06 MPa and a significant elongation at break of 80.36%. These findings suggest that the 90:5:5 formulation successfully bridges the gap between mechanical durability and the high surface area-to-volume ratio required for advanced, biodegradable wound care applications.
Keywords: chitosan; electrospinning; nanofibers; PLA; wound dressing

1. Introduction

Wound healing is an intricate and active biological process essential for restoring tissue functionality following an injury. This mechanism involves several overlapping phases, including hemostasis, inflammation, proliferation, and maturation (Asadzadeh 2024). During hemostasis, the body activates clotting mechanisms to arrest hemorrhaging, followed by the inflammatory phase, which focuses on eliminating pathogens and cellular debris. In the subsequent proliferation phase, new tissue is formed through cell migration and extracellular matrix (ECM) deposition. Finally, the maturation phase involves tissue remodeling to enhance the structural stability of the repaired area (Sonar et al. 2021). To support these stages, wound dressings play a pivotal role by protecting the site from external contaminants, maintaining an optimal microenvironment, and promoting tissue regeneration. An ideal dressing should accelerate healing while ensuring patient comfort and safety. Traditional materials like gauze or synthetic plastics have been widely used; however, plastic-based dressings raise environmental concerns due to their poor biodegradability (Wang, Wen, and Huang 2021). The accumulation of non-degradable plastic waste has necessitated the development of sustainable alternatives derived from natural polymers to mitigate long-term environmental pollution. Consequently, recent research has shifted toward eco-friendly dressings derived from biodegradable polymers. Nanofiber-based dressings have recently become a primary focus due to their biomimetic structure, which closely resembles the natural skin ECM, thereby fostering an ideal environment for tissue engineering and cell proliferation (Partovi et al. 2024). Among various These materials provide a

* Corresponding Author
Email address: belindalaulistaa@gmail.com

sustainable solution for wound recovery without exacerbating the global environmental footprint. Nanofiber-based dressings have recently become a primary focus in biomedical research due to their biomimetic structure, which closely resembles synthesis techniques, electrospinning is regarded as the most effective for producing ultrafine fibers with diameters between 5 and 100 nm. PLA is frequently utilized as a base polymer in electrospinning due to its controllable degradation and mechanical integrity (Ehyaeirad et al. 2024). Nevertheless, the inherent brittleness of PLA often limits its application. The integration of reinforcing phases, such as cellulose derived from biomass residues, serves to bridge these mechanical gaps and improve the structural stability of the resulting composites (Lestari, Anggorowati, and Hadi 2021). Given its remarkable properties, cellulose enhances the composite's tensile strength and hydrophilicity.

Furthermore, incorporating antimicrobial agents is a critical strategy in preventing infections. Chitosan, a natural biopolymer, provides intrinsic anti-inflammatory and antibacterial properties, making it an excellent functional additive. The versatility of chitosan, particularly its reactive functional groups, allows for effective modification and integration into composite matrices for various functional applications (Sulistyawati et al. 2022). Previous studies have explored various formulations; for example, Rahmayetty, 2021 found that a PLA/chitosan blend with 3% chitosan yielded optimal tensile strength of 120.396 MPa, while Madani, 2024 reported the benefits of modified cellulose in PLA-based composites for antibacterial inhibition. However, the synergistic interplay between natural cellulose and chitosan when simultaneously integrated into a PLA matrix remains to be fully elucidated. Specifically, there is a lack of research focusing on how the simultaneous addition of these two biopolymers affects the balance between surface wettability and ultrafine fiber morphology.

This study operates on the premise that the incorporation of cellulose will strengthen the structural framework of the nanofibers through mechanical reinforcement, while the addition of chitosan will refine the fiber morphology by increasing solution conductivity. By addressing this gap, this research focuses on the synthesis of a triple-component PLA/chitosan/cellulose biocomposite. Such a combination is anticipated to yield a biocomposite with a superior balance of tensile strength and ultrafine fiber diameter, ideally suited for wound dressing applications. Building on these findings, this study focuses on the synthesis of PLA/chitosan/cellulose biocomposite nanofibers via electrospinning. The primary objective is to bridge the inherent brittleness of PLA by integrating varying compositions of chitosan and cellulose. This work provides a specific contribution by optimizing a triple-component formulation that achieves the necessary flexibility and mechanical integrity for medical applications while maintaining a fully eco-friendly material profile. Ultimately, this research provides a practical scientific framework for utilizing biomass-derived additives to enhance the functional performance of biodegradable wound dressings.

2. Materials and Methods

2.1. Materials and Polymer Solution Preparation

The primary materials used in this research were PLA in pellet form, Chitosan powder, and Alpha-Cellulose. Both the Chitosan and Alpha-Cellulose were supplied by Nitra Kimia (Surabaya, Indonesia). The solvent system employed consisted of Dichloromethane (DCM) and Dimethylformamide (DMF), both of analytical grade with a purity of $\geq$ 99% and molecular weights of 84.93 g/mol and 73.09 g/mol, respectively, purchased from CV. Chemical Indonesia Multi Sentosa (Chemindo Group). All chemical reagents were used as received without further purification. In this research, PLA was utilized as the fundamental polymer matrix owing to its exceptional biocompatibility and non-toxic nature. Its renewable origin and biodegradable properties further solidify its position as a premier substrate for advanced biomedical devices and wound care systems. Although PLA exhibits good mechanical strength and processability, it is inherently brittle and possesses limited elongation at break, which may restrict its performance in flexible wound dressing applications. Therefore, PLA is commonly combined with other biopolymers to improve its functional performance. In this study, PLA was dissolved in 7 mL of DCM and homogenized using a magnetic stirrer at room temperature for 15 minutes at a stirring speed of 300 rpm to obtain a homogeneous solution, hereafter referred to as Solution A. DCM was selected as the solvent due to its excellent solubility for PLA and its suitability for electrospinning-based nanofiber fabrication. Chitosan and cellulose were incorporated as functional and reinforcing biopolymers to enhance the biological and mechanical performance of nanofiber wound dressings. Chitosan, obtained from the deacetylation of chitin, is recognized for its exceptional biological safety and hemostatic capabilities. Its intrinsic antimicrobial activity and biodegradable nature make it a versatile biopolymer for enhancing the wound recovery process.

The presence of amino ($–NH_2$) and hydroxyl (–OH) functional groups imparts a cationic character to chitosan, enabling interactions with negatively charged cell membranes and microbial walls, thereby contributing to its antibacterial activity. On the other hand, cellulose represents a highly prevalent natural polysaccharide consisting of recurring β-D-glucose monomers interconnected through glycosidic linkages. Strong intermolecular hydrogen bonding between cellulose chains results in high tensile strength, good structural stability, and excellent water retention capacity, making cellulose an effective reinforcing agent for polymer-based wound dressings. In this study, chitosan and cellulose were dissolved together in 7 mL of DMF and homogenized using a magnetic stirrer at room temperature for 15 minutes at 300 rpm to obtain a uniform solution, referred to as Solution B. DMF was selected as the solvent due to its

ISSN: 1410-394X
e-ISSN: 2460-8203

ability to facilitate the dispersion of both chitosan and cellulose in polymer blend systems intended for electrospinning. The chitosan content in Solution B was varied at 0, 2.5, 5, 7.5, and 10 wt%, while the cellulose content was adjusted to 0, 2.5, 5, and 7.5 wt%, depending on the designated sample formulation.

Subsequently, Solution A and Solution B were combined and further homogenized using a magnetic stirrer for 15 minutes at 300 rpm to ensure uniform blending of all polymer components at the molecular level. The homogeneous polymer blend solutions obtained from this process were then directly used for the fabrication of nanofiber wound dressings through the electrospinning method. The detailed compositions and corresponding sample codes are summarized in Table 1.

Table 1. Composition and Sample Codes of Nanofiber Solutions

Sample Code	PLA (wt.%)	Chitosan (wt.%)	Cellulose (wt.%)
A	100	0	0
B	90	7.5	2.5
C	90	5	5
D	90	2.5	7.5
E	90	10	0

2.2. Preparation of Nanofiber Wound Dressings by Electrospinning

The fabrication of nanofiber-based wound dressings was executed via electrospinning, owing to its operational simplicity and high efficiency in producing continuous fibers within the nanometer scale. The schematic arrangement of the electrospinning apparatus used in this study is illustrated in Figure 1. This method employs a high-voltage electrical field to counteract the surface tension of the polymer solution, which facilitates the creation of ultrafine fibers with diameters typically between 50 and 500 nm. The primary components of the electrospinning setup include a syringe for the polymer solution along with a metallic spinneret, a high-voltage power source, and a grounded collector. Structural and morphological variations in the fibers can be regulated by adjusting the spinneret design or collector setup and processing variables such as the applied voltage, flow rate, or tip-to-collector distance. The electrospinning process was conducted at a stable ambient temperature of 25°C.

Before the process began, the polymer blend was carefully loaded into a 15 mL syringe to prevent air bubble formation and installed onto an infusion pump. The solution was extruded through a 22-gauge stainless steel needle, which served as the spinneret. The needle tip was attached to the positive electrode of the power supply, while the aluminum foil collector was placed at a specific distance and connected to the negative terminal. To ensure optimal solvent evaporation and stable jet formation, the collector was placed at a fixed tip-to-collector distance of 15 cm. A constant voltage of 20 kV was applied to generate a stable electric field between the components. This electrical force caused the polymer solution to form a Taylor cone and emerge as a charged jet directed toward the collector. As the jet traveled, solvent evaporation occurred, resulting in the accumulation of solid nanofiber membranes on the collector surface. The extrusion was maintained at a steady flow rate of 7 mL/h until the entire volume of the polymer solution was fully utilized. These specific parameters were strictly controlled to maintain consistency in fiber diameter and morphology across all samples.

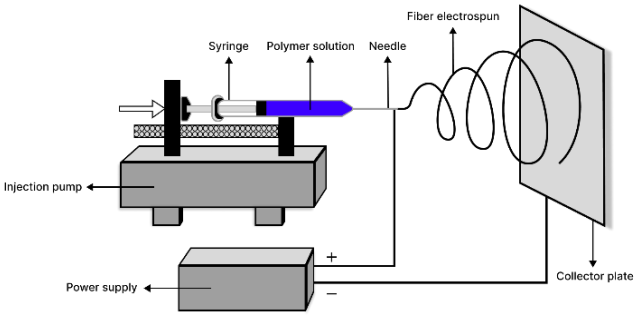

Figure 1. Schematic of the electrospinning system

2.3. Characterization and Testing of Nanofibers

Contact Angle analysis

The surface wettability characteristics of the nanofiber wound dressings were determined through contact angle analysis employing the sessile drop technique. These observations were conducted using a contact angle goniometer integrated with a high resolution digital camera to ensure precise measurement of the droplet interaction with the membrane surface. Prior to testing, the nanofiber samples were gently cleaned with a dry, lint-free cloth to remove surface contaminants. A droplet of deionized water with a fixed volume of 0.01 mL was carefully deposited onto the nanofiber surface using a micropipette or a 1 mL syringe. The droplet profile was captured immediately after deposition, and the contact angle was determined from the recorded images using ImageJ software (v1.52). To ensure data reliability and reproducibility, contact angle measurements were conducted at five different locations (n=5) for each sample. The results are reported as the mean value along with the corresponding standard deviation (SD). Surface wettability was classified based on contact angle values, where contact angles below 90° indicate hydrophilic surfaces and contact angles above 90° indicate hydrophobic surfaces.

2.3.1. Scanning electron microscopy (SEM)

The investigation of surface morphology and fiber architecture including diameter distribution was conducted using a HITACHI FLEXSEM 100 scanning electron

microscope which featured a secondary electron (SE) detector. To enhance surface conductivity for clearer imaging the nanofiber specimens were secured onto aluminum stubs and underwent a sputter-coating process before analysis. Observations were performed at multiple magnifications between 500× and 10,000× to assess the overall fiber uniformity while identifying potential imperfections such as bead formation or fiber fusion. Furthermore ImageJ software (v1.52) was employed to process the SEM micrographs. The average fiber diameter was determined by measuring 20 random fibers (n=20) from the micrographs for each experimental group. The diameter distribution and uniformity were analyzed and expressed as mean ± standard deviation (SD).

2.3.2. Fourier Transform Infrared (FTIR) Analysis

To examine molecular interactions and identify functional groups within the PLA/chitosan/cellulose biocomposites Fourier Transform Infrared (FTIR) spectroscopy was performed using a Shimadzu FTIR-8400S instrument. This analytical technique relies on the infrared radiation absorption by molecular bonds which generates specific peaks representing the functional groups present in the material. The resulting spectra were scrutinized to verify the characteristic chemical groups of PLA, chitosan, and cellulose while investigating potential intermolecular phenomena such as hydrogen bonding between the integrated polymer phases.

2.3.3. Mechanical Properties Analysis

The mechanical robustness of the fabricated dressings was assessed through tensile evaluation utilizing a universal testing machine (UTM) following standardized protocols for material testing. Parameters such as tensile strength, Young's modulus, and elongation at break were recorded to represent the strength, stiffness, and ductility of the composites respectively. High-quality mechanical performance is a prerequisite for wound care materials as it dictates the durability and flexibility required to withstand deformation during clinical use. Additionally the study analyzed how polymer ratios and the inclusion of reinforcing agents impacted the tensile behavior since modifications in fiber-reinforced systems are known to alter mechanical properties significantly.

2.4. Data Analysis and Statistical Treatment

The quantitative results from the WCA and SEM measurements were analyzed statistically to ensure data reliability. The arithmetic mean ($\bar{x}$) and standard deviation (σ) were calculated using the following equations:

$$\bar{x} = \frac{\sum_{i=1}^{n} x_i}{n} \quad (1)$$

$$\sigma = \sqrt{\frac{\sum_{i=1}^{n} (x_i - \bar{x})^2}{n-1}} \quad (2)$$

Where :

- $\bar{x}$: mean
- x_i : individual value
- n : total number of repetition (5 for WCA ; n 20 for fiber diameter (SEM))
- σ : standard deviation (SD)

Unit and Analysis :

- Fiber diameter : measured in nanometers (nm)
- Contact angel : measured in degrees (°)
- Mechanical Properties : tensile strength (MPa)
  elongation at break (%)

3. Results and Discussion

3.1. Contact Angle of Nanofiber Wound Dressings

The variation in material composition plays a significant role in determining the hydrophobicity of nanofiber mats. This property is measured by the contact angle (°), which is a key parameter for wound dressing applications, as a more hydrophobic surface can prevent water penetration while maintaining a moist wound environment (Madani et al. 2024). Based on five-fold measurements (n=5), sample code A exhibited the highest contact angle of 103.778° ± 10.15°, reflecting the intrinsic highly hydrophobic nature of PLA. This behavior is attributed to the dominance of nonpolar ester groups in the PLA structure, which reduces interactions with water molecules (Rahmayetty et al. 2021).

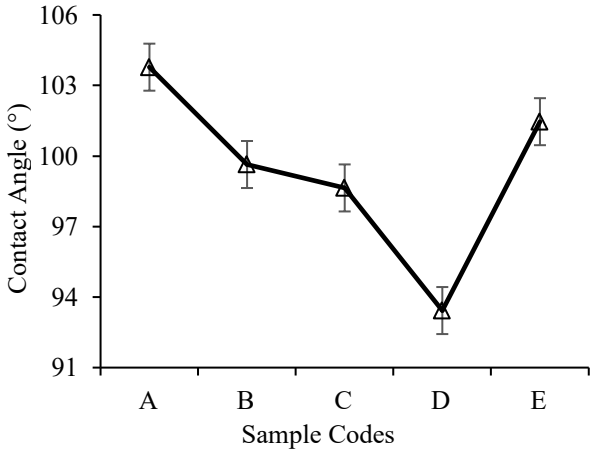

Figure 2. Effect of material composition on contact angle values of nanofiber wound dressings

When PLA is combined with chitosan and cellulose (codes B–E), the contact angle decreases, indicating an increase in the surface hydrophilicity of the nanofibers. Samples E (PLA + chitosan) and B maintained relatively high values (101.459° ± 3,42° and 99.638° ± 3,02°) due to the dominance of chitosan, whereas codes C and D showed a more pronounced decrease (98.642° ± 2,29° and 93.426° ± 2,84°) due to a higher proportion of cellulose The reduction in contact angle is driven by the abundant polar functional groups, specifically the hydroxyl (–OH) groups in cellulose and amine (–NH_2) groups in chitosan. These groups act as hydrophilic sites that facilitate the formation

ISSN: 1410-394X
e-ISSN: 2460-8203

of hydrogen bonds with water droplets, thereby increasing the surface free energy of the nanofibers. Furthermore, the synergistic effect of cellulose in sample D suggests a higher density of these oxygen-containing functional groups on the fiber surface, which effectively attracts water molecules and reduces the interfacial tension between the liquid and the solid surface (Asadzadeh 2024; Njuguna, Muriuki, and Karenga 2022).

3.2. Morphological Characteristics and Fiber Diameter Analysis (SEM)

The morphology of nanofibers in samples A and C was analyzed at 20 kV using SEM to evaluate the effect of material composition on fiber diameter, uniformity, and surface structure.

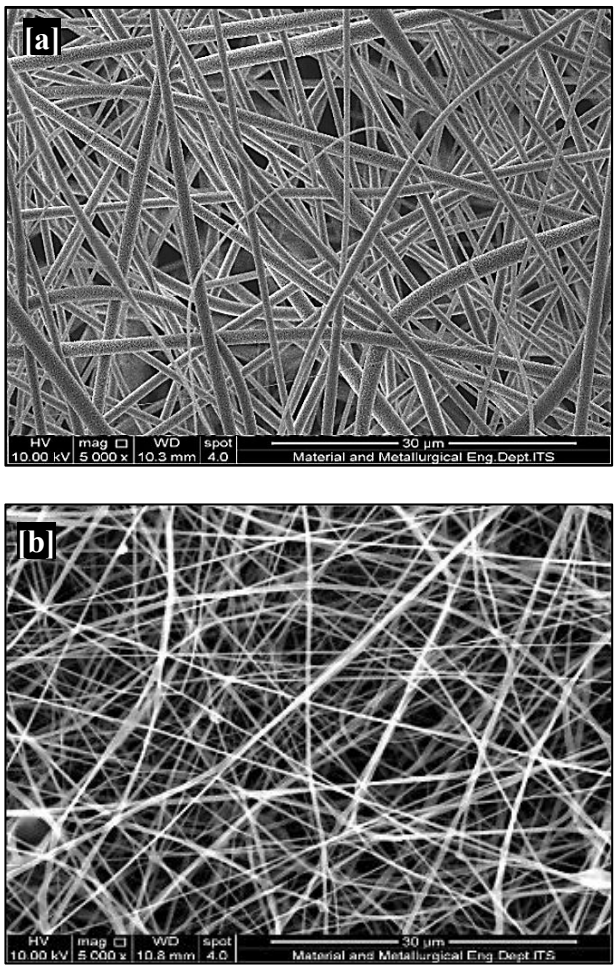

Figure 3. SEM image of Nanofiber (a) code A; (b) code C

SEM images at 5000× magnification revealed differences in morphology and the presence of defects such as beads. Based on the measurement of 20 random fibers (n=20) for each group, Sample A (PLA) exhibited an average fiber diameter of 517.12 ± 57,33 nm, with thick, uniform fibers free of beads, due to high solution viscosity and hydrophobicity that maintained jet stability. Sample C (PLA/ chitosan /cellulose) had a smaller average diameter of 329.68 ± 31,00 nm. The inclusion of standard deviation reflects the narrow diameter distribution, indicating high fiber uniformity. The hydroxyl groups in cellulose and amine groups in chitosan increased the solution polarity and electrical conductivity. This increase in conductivity enhances the net charge density carried by the electrospinning jet, resulting in stronger electrostatic stretching forces during the whipping process. Consequently, the polymer jet undergoes more extensive thinning before reaching the collector, which leads to the formation of finer nanofibers. The balanced proportion of the two biopolymers maintained fiber quality, producing smooth nanofibers with a consistent diameter distribution and no defects as the added biopolymers also influenced the solution viscosity to stay within the optimal range for stable jet formation (Pais et al. 2022)

3.3. Functional Group Analysis of Nanofibers (FTIR)

FTIR analysis was performed to identify functional groups in nanofibers of samples A and C and to observe chemical changes resulting from the incorporation of cellulose and chitosan into the PLA matrix. Sample A (pure PLA) served as a control to show the characteristic PLA peaks, while sample C was selected due to the balanced proportion of cellulose and chitosan, allowing for clear observation of the uniform distribution of polar functional groups.

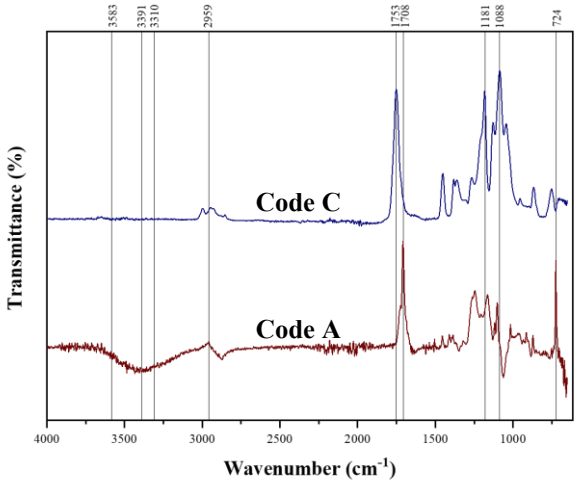

Figure 4. FTIR Spectrum of Nanofibers

The FTIR spectrum of sample C showed significant changes compared to pure PLA. The 3310–3583 cm^{-1} region, representing –OH and $–NH_2$ groups, appeared stable and consistent, indicating a homogeneous distribution of hydrophilic groups from cellulose and chitosan (Nandiyanto, Ragadhita, and Fiandini 2023). The broadening of this peak in Sample C suggests the formation of intermolecular hydrogen bonds between the hydroxyl groups of cellulose and the amino groups of chitosan with the carbonyl groups of PLA. The intensity of the 2959 cm^{-1}

band, associated with aliphatic –CH groups, decreased in sample C due to the contribution of polar groups from the biopolymers. Increased intensities at 1753 cm^{-1} and 1181 cm^{-1} indicate additional C=O and C–O–C groups from cellulose and chitosan, while the 1088 cm^{-1} band confirms overlapping absorptions from all three components. The slight shift in the C=O stretching vibration at 1753 cm^{-1} further confirms the chemical compatibility and molecular interaction within the ternary blend. The weak band at 724 cm^{-1} reflects the reduced dominance of aliphatic –CH groups in PLA due to biopolymer addition. Overall, these spectral changes confirm the successful incorporation of cellulose and chitosan and chemical interactions between polymer chains, which can influence the mechanical properties, biodegradability, and bioactivity of the nanofibers, demonstrating that the intermolecular cross-linking through physical interactions produces a more functional and stable polymer matrix (Asadzadeh 2024).

3.4. Mechanical Properties of Nanofiber Wound Dressings

The mechanical properties of the nanofiber wound dressings with various material compositions are presented in Figure 5. The yield strength represents the stress level at which the material begins to deform plastically.

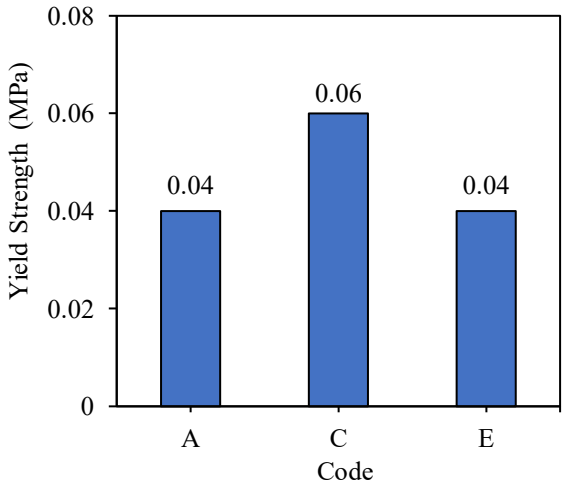

Figure 5. Yield strength of nanofiber with different material compositions

As shown in Figure 5, Sample A (pure PLA) and Sample E (PLA/chitosan) both exhibited a yield strength of 0.04 MPa, while Sample C (PLA/chitosan/ cellulose) showed a higher value of 0.06 MPa. The superior yield strength of Sample C can be attributed to the reinforcing effect of cellulose within the composite matrix. As a high-strength natural polymer, cellulose nanofibers act as structural 'pillars' that restrict the molecular mobility of the PLA chains, thereby increasing the resistance of the material against deformation (Mokhena et al. 2021). This reinforcement is made possible by the chemical compatibility observed in the FTIR spectra. The intermolecular hydrogen bonding—indicated by the OH and NH_2 peaks in the 3310–3583 cm^{-1} region—functions as a molecular bridge that facilitates efficient stress transfer from the PLA matrix to the cellulose reinforcements. Furthermore, the significant reduction in fiber diameter observed in the SEM analysis for Sample C (329.68 ± 31.00 nm) compared to Sample A (517.12 ± 57.33 nm) plays a crucial role. Finer nanofibers typically possess a higher degree of molecular orientation and crystallinity along the fiber axis, which enhances their mechanical integrity. In contrast, Sample E did not show an increase in yield strength over Sample A, suggesting that the addition of chitosan alone, without the structural support of cellulose, is insufficient to significantly bolster the mechanical resistance of the PLA matrix. Therefore, the ternary combination in Sample C creates a more integrated and robust biocomposite structure through the synergistic effect of physical cross-linking and improved fiber morphology.

3.5. Effect of Material Composition on the Tensile Strength of Nanofiber

The tensile strength results for the various nanofiber compositions are illustrated in Figure 6. Variations in material composition significantly dictate the tensile strength of the nanofibers, where Sample A (pure PLA) exhibits the highest value of 0.43 MPa, while Samples C and E show lower values of 0.21 MPa and 0.23 MPa, respectively.

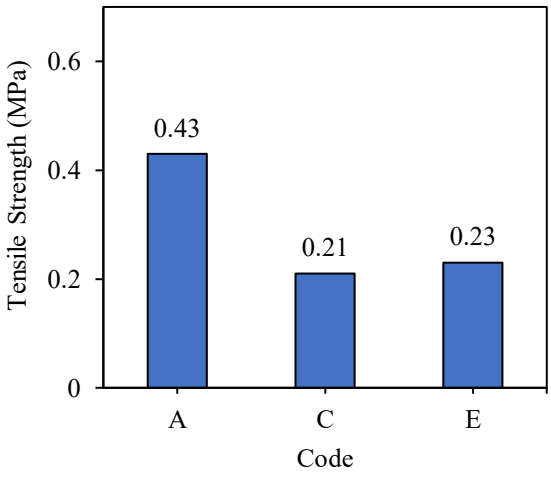

Figure 6. Tensile strength of nanofiber with different material compositions

The superior strength of Sample A is associated with the inherent semi-crystalline structure of pure PLA, which allows for effective resistance against tensile loads. However, the reduction in tensile strength for Sample C and E suggests that the incorporation of biopolymers induces a structural transition within the fiber matrix. Chemically, this is supported by the FTIR spectra, where the emergence of polar –OH and $–NH_2$ bands indicates the presence of cellulose and chitosan. While these groups facilitate some intermolecular hydrogen bonding, their presence simultaneously disrupts the original crystalline

ISSN: 1410-394X
e-ISSN: 2460-8203

order and molecular chain alignment of the PLA backbone (Mokhena et al. 2021). The decrease in strength in Sample C (0.21 MPa) compared to Sample A is primarily due to interfacial heterogeneity between the hydrophobic PLA and the hydrophilic biopolymers. This incompatibility can lead to 'stress concentration sites' at the interfaces of the polymer blends, where the mechanical load is not distributed uniformly, leading to earlier failure under tension. Furthermore, the disruption of the aliphatic –CH groups (2959 cm^{-1}) observed in FTIR confirms that the biopolymers interfere with the dense packing of PLA chains. Although Sample E (0.23 MPa) shows a slightly higher strength than Sample C, both are lower than pure PLA, indicating that while the functional groups add bioactivity, they act as structural discontinuities that reduce the peak tensile resistance of the composite nanofibers (Asadzadeh, 2024).

3.6. Effect of Material Composition on the Young's Modulus of Nanofiber

The impact of PLA, chitosan, and cellulose compositions on the Young's Modulus of the nanofibers is illustrated in Figure 7. This parameter indicates the stiffness of the material and its resistance to elastic deformation.

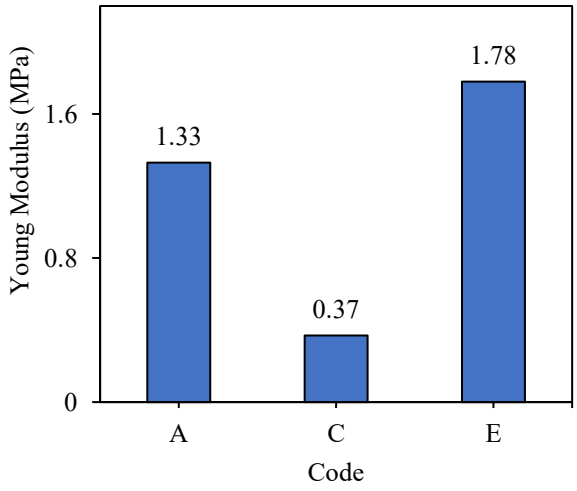

Figure 7. Young Modulus of nanofiber with different material compositions

As shown in Figure 7, Sample E exhibits the highest stiffness at 1.78 MPa, followed by Sample A at 1.33 MPa, and Sample C at the lowest value of 0.37 MPa. The superior rigidity of Sample E is chemically supported by the FTIR spectrum, where the interaction between the amino groups of chitosan and the PLA matrix promotes a more rigid molecular framework. Mechanically, this is attributed to the strong interfacial adhesion between the amine groups of chitosan and the PLA matrix, which restricts the elastic deformation of the polymer chains under low strain. Chemically, this interaction is supported by the specific hydrogen bonding observed in the FTIR spectra, which acts as a physical cross-link that enhances the overall modulus of the composite. In contrast, Sample C (PLA/chitosan/cellulose) showed a substantial decrease in stiffness to 0.37 MPa. The presence of cellulose in this ternary blend appears to disrupt the crystalline continuity of the PLA matrix, leading to a more compliant and flexible structure. This reduction in modulus occurs because the high density of biopolymer integration—as indicated by the broad –OH and $–NH_2$ bands (3310–3583 cm^{-1})—facilitates interphase heterogeneity (Asadzadeh 2024). Instead of providing rigid reinforcement, the cellulose fibers in this specific composition may act as 'spacers' that increase the free volume between PLA chains, thereby reducing the force required for elastic stretching. These results align with Madani (2024), who reported that while chitosan can enhance rigidity through specific molecular interactions, the incorporation of cellulose can sometimes reduce stiffness by forming a less homogeneous and more flexible network within the hydrophobic polymer matrix.

3.7. Effect of Material Composition on the Maximum Force Resistance of Nanofiber

The maximum force values for the nanofiber wound dressings across various material compositions are summarized in Figure 8. This parameter indicates the peak load the material can withstand before structural failure occurs.

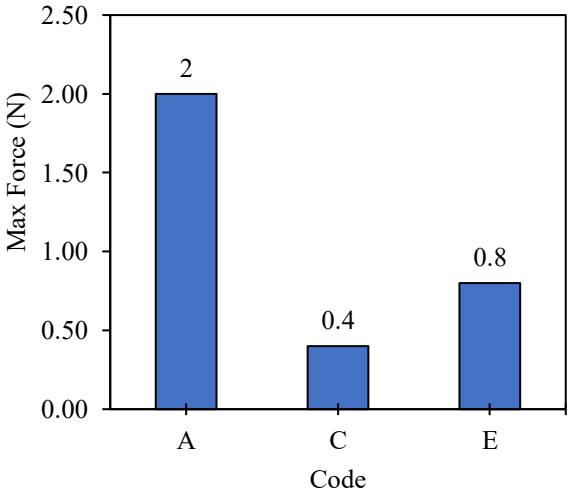

Figure 8. Max Force of nanofiber with different material compositions

Variations in material composition significantly affect the maximum force obtained during mechanical testing, with Sample A (pure PLA) showing the highest value of 2 N, followed by Sample E with 0.8 N, and Sample C exhibiting the lowest value of 0.4 N. The superior maximum force of Sample A is attributed to the well-ordered and continuous polymer chain structure of pure PLA, which facilitates efficient and uniform load

distribution across the fiber. However, the incorporation of biopolymers leads to a significant reduction in the load-bearing capacity. In Sample C (0.4 N), the presence of both cellulose and chitosan disrupts the original viscoelasticity and molecular continuity of the PLA matrix. Mechanically, this suggests that the biopolymers may act as structural discontinuities or 'impurities' within the PLA backbone, potentially introducing microvoids or interfacial weak points that promote premature failure under stress. This structural disruption is chemically supported by the FTIR spectra, where the emergence of broad –OH and –NH_2 peaks (3310–3583 cm^{-1}) indicates the successful integration of hydrophilic components. However, the decreased intensity of the aliphatic –CH band at 2959 cm^{-1} confirms that these biopolymers interfere with the dense packing of the PLA chains. As a result, the mechanical load is not effectively distributed, leading to a lower force threshold before the fiber structure reaches its breaking point. These results are consistent with Asadzadeh (2024), who reported that while biopolymer addition increases the functional properties of the nanofibers, it often reduces the overall load-bearing capacity due to structural heterogeneity and poor filler dispersion compared to the homogeneous pure PLA control.

3.8. Effect of Material Composition on the Elongation Behavior of Nanofiber

The elongation properties of the nanofiber wound dressings across various material compositions are displayed in Figure 9. This parameter determines the material's ability to stretch and deform before breaking, which is a critical factor for wound dressing flexibility.

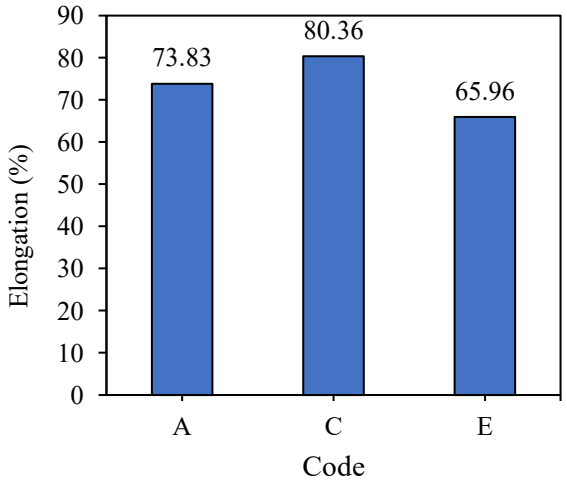

Figure 9. Elongation of nanofiber with different material compositions

Variations in material composition significantly affect the elongation of the nanofibers, which determines the material's ability to stretch before breaking. Based on the experimental results, Sample A exhibited an elongation of 73.83%, Sample E showed a decrease to 65.96%, and Sample C reached a peak value of 80.36%. The superior elongation observed in Sample C is attributed to the synergistic effect of combining cellulose and chitosan within the PLA matrix. Mechanically, the integration of these biopolymers acts as a 'molecular lubricant' or plasticizing agent that enhances the mobility of the PLA chains. This allows the polymer network to undergo greater plastic deformation and stretching before structural failure occurs (Latifa et al. 2024). This behavior is chemically supported by the FTIR spectrum of Sample C, where the broad intensity in the 3310–3583 cm^{-1} region indicates an extensive intermolecular hydrogen-bonding network. These hydrogen bonds function as flexible 'chemical bridges' that facilitate better chain sliding and deformability compared to the more rigid and brittle structure of pure PLA. Conversely, the decrease in elongation for Sample E (65.96%) suggests that the addition of chitosan alone restricts polymer chain mobility. Without the structural support and spacing provided by cellulose, the chitosan particles may act as rigid obstacles within the PLA matrix, increasing the brittleness and leading to earlier fracture. These results align with Asadzadeh (2024), confirming that the ternary combination in Sample C creates a more integrated and flexible biocomposite structure. This enhanced elongation is particularly beneficial for wound dressing applications, as it provides the necessary flexibility to conform to body contours and movements while maintaining structural integrity.

4. Conclusions

This study successfully developed biodegradable PLA/chitosan/cellulose biocomposite nanofibers through electrospinning, optimized for wound dressing applications. The research establishes that the synergistic integration of 5 wt% chitosan and 5 wt% cellulose (Sample C) significantly enhances the functional performance of the PLA matrix. The primary contribution of this work is the identification of an optimal ternary blend that balances surface wettability and mechanical flexibility, addressing the inherent brittleness of pure PLA. Key findings demonstrate that Sample C achieved a contact angle of 98.64°, providing a moderately hydrophobic surface ideal for maintaining a moist wound environment. Morphological analysis revealed a significant reduction in average fiber diameter from 517.12 nm (pure PLA) to 329.68 nm (Sample C), resulting in a more uniform and bead-free structure. Most importantly, the mechanical evaluation confirmed that the developed biocomposite outperformed pure PLA in ductility, exhibiting a peak elongation of 80.36% and a yield strength of 0.06 MPa. While pure PLA showed higher tensile strength, the improved elasticity and structural integrity of Sample C make it more suitable for dynamic wound coverage. This research provides a clear structure-property framework for developing high-performance biopolymer nanofibers. The optimized PLA/chitosan/cellulose system offers a superior combination of wettability control, molecular compatibility, and mechanical reliability, making it a

ISSN: 1410-394X
e-ISSN: 2460-8203

promising candidate for advanced biodegradable wound dressings.

Acknowledgments
The author would like to express sincere gratitude to the Department of Chemical Engineering, Institut Teknologi Sepuluh Nopember (ITS), for providing the necessary laboratory facilities, as well as a supportive academic environment that facilitated the implementation of this research.

Special and deepest appreciation is extended to Prof. Dr. Ir. Tri Widjaja, M.Eng. for his invaluable guidance, technical feedback, and for conceptualizing the original research idea. This study was fully funded and supported through the research grant led by Prof. Dr. Ir. Tri Widjaja, M.Eng. at the Institut Teknologi Sepuluh Nopember. His mentorship was instrumental throughout the development of the preparation of this manuscript.

The author is also grateful to the laboratory staff and fellow undergraduate students for their technical assistance, administrative support, and for their help during the experimental and data collection phases.

Statement

During the preparation of this work, the authors used Gemini in order to improve English language clarity and proofread the manuscript. After using this tool, the authors reviewed and edited the content as needed and take full responsibility for the scientific content of the publication. No part of the scientific analysis, data processing, modelling, or interpretation was generated by AI. All scientific content, results, and conclusions were fully produced and verified by the authors.

Credit authorship contribution statement

Belinda Laulista: Writing – original draft, Formal analysis, Investigation, Data curation, Methodology, Software, Review & Editing, : Conceptualization
Desy Miftachul: Writing, Methodology, Validation, review & editing
Lilik Suprianti: : Conceptualization, Resources, Writing – review & editing, Supervision, Project administration.
Tri Widjaja : Conceptualization, Funding acquisition, Resources, Supervision, Project administration.
Aisyah Alifatul Zahidah Rohmah : Conceptualization, Methodology.
Citra Yulia Sari : Conceptualization, Methodology, Data curation.

Declaration of competing interest

The authors declare that they have no known competing financial interests or personal relationships that could have appeared to influence the work reported in this paper.

Data availability
All data generated or analyzed during this study, including experimental results, tensile strength measurements, and antimicrobial inhibition zones, are fully included in this published article.

References

Asadzadeh, F. (2024). Assessing Polylactic Acid Nanofibers with Cellulose and Chitosan Nanocapsules Loaded with Chamomile Extract for Treating Gram-Negative Infections. *Scientific Reports : 14, 1, 1–13*. doi:10.1038/s41598-024-72398-9.

Ehyaeirad, Negin, Nima, B., Masoomeh, D., & Leila, S. R. (2024). Polylactic Acid Films Incorporated with Nanochitosan, Nanocellulose, and Ajwain Essential Oil: Synthesis, Characterizations, with In-Vitro and In-Vivo Antimicrobial Properties for Infected Wound Healing. *Carbohydrate Polymer Technologies and Applications*, *7*, 1–11. doi:10.1016/j.carpta.2024.100425.

Latifa, Annisa, C., Dewi, P., Indriana, L., & Fauzan, I. (n.d.). embuatan Bioplastik Dari Pati Umbi Ganyong Menggunakan Penguat Seng Oksida Dan Plastilizer Gliserol Dengan Metode Melt Intercalation Synthesis of Ganyong Starch-Based Bioplastic with Zinc Oxide Filler and Glycerol Plasticizer via Melt Intercalation Method. *21*(2), 122–32.

Lestari, Indriana, Heni, A., & Faizah, H. (2021). fek Pretreatment Ultrasonikasi Terhadap Hidrolisis Enzimatis Spirulina Platensis Residue The Effects of Ultrasonication Pretreatment to Enzymatic Hydrolysis of Spirulina. *Platensis Residue*, *18*(1), 24–28.

Madani, Maryam, Cristiana, D., Zahra, G., Hossein, B., Päivi, T., Timo, L., Jukka, N., & Jukka, S. (2024). Functionalized Cellulose Nanocrystals Reinforced PLA-Gelatin Electrospun Fibers for Potential Antibacterial Wound Dressing and Coating Applications. *nternational Journal of Biological Macromolecules*, *287*, 1-12. doi:10.1016/j.ijbiomac.2024.138389.

Mokhena, Sefadi, Sadiku, John, Mochane, M., & Mtibe, A. (2021). Thermoplastic Processing of PLA/Cellulose Nanomaterials Composites. *Polymers*, *10*(12), 2-29. doi:10.3390/polym10121363.

Nandiyanto, Asep, B., Risti, R., & Meli, F. (2023). Interpretation of Fourier Transform Infrared Spectra (FTIR): A Practical Approach in the Polymer/Plastic Thermal Decomposition. *Indonesian Journal of Science and Technology*, *8*(1), 113-26.

doi:10.17509/ijost.v8i1.53297.

Njuguna, Mwaura, J., Mary, M., & Samuel, K. (2022). Attenuated Total Reflectance –Fourier Transform Infrared (ATR-FTIR) Analysis of Ocimum Kenyense Essential Oils. *International Journal of Pure and Applied Chemistry*, *1*(1), 1-10. doi:10.37284/ijpac.1.1.722.

Pais, Vânia, Miguel, N., Catarina, G., Rui, M., & Raul, F. (2022). Hydrophobic Performance of Electrospun Fibers Functionalized With TiO2 Nanoparticles. *extile Research Journal*, *92*(15-16), 2719-30. doi:10.1177/00405175211010669.

Partovi, Alireza, Mostafa, K., Sareh, A., Sayed, O., & Ranaei, S. (2024). Electrospun Nanofibrous Wound Dressings with Enhanced Efficiency Through Carbon Quantum Dots and Citrate Incorporation. *Scientific Reports*, *14*(1), 1-12. doi:10.1038/s41598-024-70295-9.

Rahmayetty, Endarto, Y., Alfirano, & Nufus, K. (2021). The Effect of Cellulose Nanocrystaline Blending to the Mechanical Properties of Composite Edible Film (PLA/CNC). *Joint proceedings of the 2nd and the 3rd International Conference on Food Security Innovation*, *9*, 100-107. doi:10.2991/absr.k.210304.018.

Sonar, Sanjay, P., Naveena, A., Nasheed, A., Ashok, M., & Deepak, T. (2021). A Comprehensive Review on Wound Dressing Usage in Clinical Settings. *International Journal of Surgery and Medicine*, *8*(3), 16-26. doi:10.5455/ijsm.136-1648103567.

Sulistyawati, Endang, Heni, A., Nadia, R., & Navyta, A. (2022). Isoterm Dan Termodinamika Adsorpsi Mikrokapsul Kitosan Tertaut Silang Kalium Persulfat Terhadap Zat Warna Methyl Orange Isotherm and Adsorption Thermodynamics Cross-Linked Chitosan Microcapsules of Kalium Pershulphate to Methyl Orange Dye. *19*(2), 51-57.

Wang, Yu, Wen, & Yi, H. (n.d.). A Study on Modification of Polylactic Acid and Its Biomedical Application. *E3S Web of Conferences*, *308*. doi:10.1051/e3sconf/202130802008.